

10-14 July 2016, Vienna, Austria

# Optical Breath Gas Extravehicular Activity Sensor for the Advanced Portable Life Support System

William R. Wood<sup>1</sup>, Miguel E. Casias<sup>2</sup> and Jeffrey S. Pilgrim<sup>3</sup>  
*Vista Photonics, Inc., Las Cruces, NM 88001*

Cinda Chullen<sup>4</sup> and Colin Campbell<sup>5</sup>  
*NASA Johnson Space Center, Houston, TX, 77058*

The infrared gas transducer used during extravehicular activity (EVA) in the extravehicular mobility unit (EMU) measures and reports the concentration of carbon dioxide (CO<sub>2</sub>) in the ventilation loop. It is nearing its end of life and there are a limited number remaining. Meanwhile, the next generation advanced portable life support system (PLSS) now being developed requires CO<sub>2</sub> sensing technology with performance beyond that presently in use. A laser diode (LD) spectrometer based on wavelength modulation spectroscopy (WMS) is being developed to address both applications by Vista Photonics, Inc. Accommodation within space suits demands that optical sensors meet stringent size, weight, and power requirements. Version 1.0 devices were delivered to NASA Johnson Space Center (JSC) in 2011. The sensors incorporate a laser diode based CO<sub>2</sub> channel that also includes an incidental water vapor (humidity) measurement. The prototypes are controlled digitally with a field-programmable gate array (FPGA)/microcontroller architecture. Version 2.0 devices with improved electronics and significantly reduced wetted volumes were delivered to JSC in 2012. A version 2.5 upgrade recently implemented wavelength stabilized operation, better humidity measurement, and much faster data analysis/reporting. A wholly reconfigured version 3.0 will maintain the demonstrated performance of earlier versions while being backwards compatible with the EMU and offering a radiation tolerant architecture.



<sup>1</sup>Senior Research Engineer, 4611 Research Park Circle, B220, Las Cruces, New Mexico 88001-5948.

<sup>2</sup>Senior Research Engineer, 4611 Research Park Circle, B220, Las Cruces, New Mexico 88001-5948.

<sup>3</sup>President, 4611 Research Park Circle, B220, Las Cruces, New Mexico 88001-5948.

<sup>4</sup>Project Engineer, Space Suit and Crew Survival Systems Branch, Crew and Thermal Systems Division, 2101 NASA Parkway, Houston, Texas 77058, Mail code EC5.

<sup>5</sup>PLSS Lead, Space Suit and Crew Survival Systems Branch, Crew and Thermal Systems Division, 2101 NASA Parkway, Houston, Texas, 77058, Mail code EC5.

## I. Introduction

THE infrared gas transducer developed for the external mobility unit to measure and report the concentration of carbon dioxide in the ventilation loop during EVA is approaching its end of life. Replacements are no longer available and existing devices are showing their age. Next generation advanced portable life support systems require next generation breath gas sensing technology with performance beyond that in use on the EMU. The high-performance optical sensors being developed must meet stringent size, weight, and power requirements if they are to be backwards compatible with the EMU. There may be some flexibility in forward looking devices for the advanced PLSS. Optical sensors based on laser spectroscopy are being developed for the advanced PLSS with backwards EMU compatibility by Vista Photonics.

Two prototype version 1.0 devices were delivered to NASA JSC in September 2011, Fig. 1. The sensors incorporate a semiconductor laser based carbon dioxide channel that also includes an incidental water vapor (humidity) measurement and a separate oxygen channel using a VCSEL. Both prototypes are controlled with a low-power digital architecture. Based on the results of the initial instrument development, further prototype development and refinement were desired. Several improvements to the version 1.0 devices were implemented and the upgraded version 2.0 devices were delivered to NASA in July 2012 (title page photo). The combination of low power digital control electronics with the performance of infrared laser optical measurements enables multi-gas sensors with significantly increased performance over that presently offered in the EMU. One of the devices was recently upgraded as version 2.5 by implementing laser wavelength locking to eliminate drift encountered in previous versions.

Optical absorption spectroscopy provides signal that is linear and quantitative in concentration of the absorbing species for small absorbance. As expressed by Beer's law, the signal is directly proportional to the concentration. WMS allows measurement of weak optical absorbance by shifting the detection band to high frequencies, where laser excess ( $1/f$ ) noise is reduced. WMS offers a sensitivity enhancement over direct optical absorption spectroscopy of a factor between 100 and 1000.

To implement WMS, a small amplitude modulation at frequency  $f$  is superimposed on the laser diode injection current causing modulation of the laser wavelength, because wavelength is tuned by changing the current. The amplitude of the current modulation is chosen so that the induced wavelength modulation is comparable to the width of the spectral feature under study. Absorption by the target gas converts the laser wavelength modulation to an amplitude modulation that induces AC components in the detector photocurrent. Phase-sensitive electronics are then used to demodulate the detector photocurrent at a selected harmonic,  $nf$  (typically,  $n = 2$ ), Fig. 2. By implementing this technique at sufficiently high frequencies,  $1/f$  laser noise is reduced and occasionally detector-limited sensitivity can be achieved.



**Figure 1. Version 1.0 APLSS Optical Sensor.** The nearly cubic shape met the footprint requirements sought at the time of the development.

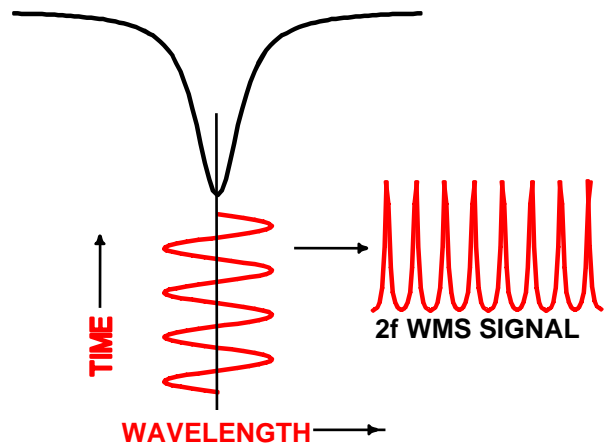


**Figure 2. Generation of WMS signal.** Modulation of an optical source wavelength across the center of a molecular absorption feature produces WMS signal at twice the modulation frequency.

The infrared wavelength range is well suited for both sensitive and selective detection of carbon dioxide and water vapor because many isolated absorption features are available for both species. Careful selection of the nominal wavelength range can even result in both species being detected with a single laser device. While current modulation and second harmonic detection provide the basic absorption signal at a single wavelength, simultaneous current or temperature tuning the laser wavelength at a lower rate can produce either a single isolated absorption feature or an entire spectrum. Figure 3 shows the spectrum obtained for carbon dioxide and water vapor in the

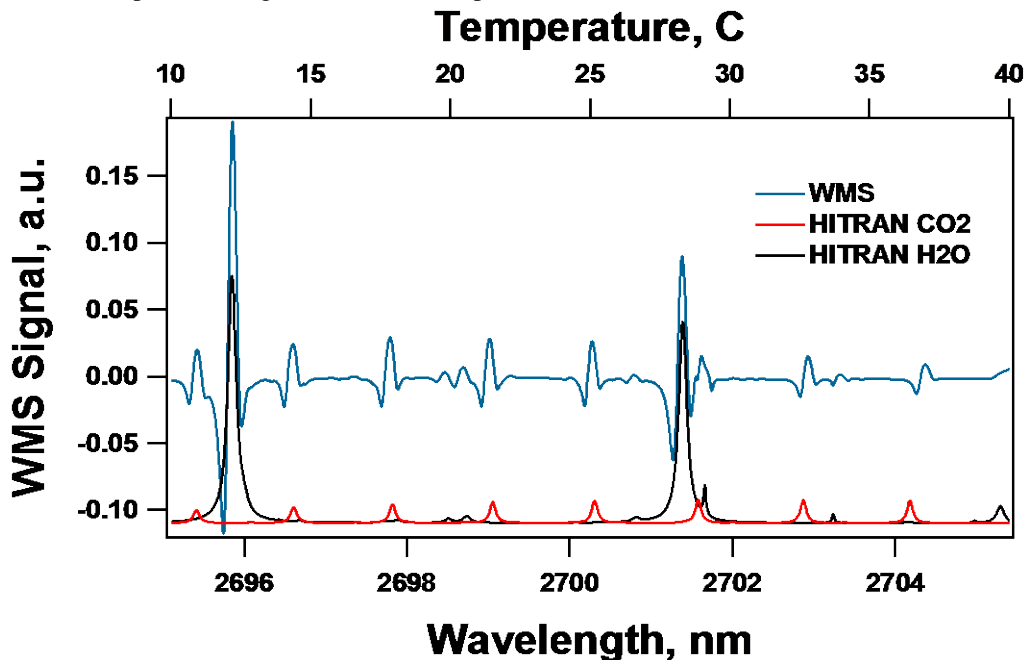


**Figure 3.** *2f WMS spectrum in 2700 nm range. Ambient CO<sub>2</sub> and moisture absorption at 600 Torr for a 25 cm open path. The top axis shows how the laser wavelength is tuned with temperature.*

selected 2700 nm wavelength range along with a comparison to the HITRAN spectral database. The spectrum in the figure was obtained by slowly changing the laser temperature using a built-in thermoelectric cooler (TEC) over a span of about 30 °C. Within the wavelength range produced by that scan there are eight strong carbon dioxide absorption features and numerous water vapor lines of varying strength. The sensors for the APLSS application operate at the 2703 nm region where lines from both species can be accessed with a simple laser current ramp.

## II. Optical Sensor Version 1.0

Many improvements had to be implemented in order to arrive at the final design of the version 1.0 sensors and knowledge was applied from various Phase II SBIR projects. The result was an amalgam of optical approaches for the CO<sub>2</sub> and O<sub>2</sub> channels that were not the ones originally demonstrated to the stakeholders at NASA JSC who ultimately funded the Phase III development.

The challenge was to integrate the optical channels into a small rugged device that operates autonomously. This required a reduction in size of both originally envisioned optical layouts as well as all the associated electronics. Design integration and electronics reduction occurred over the course of three months. The version 1.0 sensors made some design concessions to meet the timeline. An expeditious compromise was to simply co-locate both sensor channels into the same enclosed volume, but without the control electronics, for gas sampling at variable pressure. Consequently, the enclosed volume of 200 cm<sup>3</sup> was still much larger than required to simply house each channel separately. The black box on top in Fig. 1 with the electronic feed throughs houses both of the optical channels.

The electronics architecture in the 1.0 devices is comprised of one main analog board, an FPGA board, and a microcontroller. Design of the main analog board was straightforward after drawing on the experience acquired in a Phase III development of Vista Photonics' Multi-Gas Monitor (MGM) presently having operated for over two years on ISS. MGM operates four independent laser channels. The function of the main analog board is to provide current drive capability for both laser channels and control their associated TECs. An additional TEC circuit is used to control the photodetector temperature for the CO<sub>2</sub> channel. The main board also routes power to the FPGA and microcontroller boards and two small photodetector preamplifiers. The optical enclosure dictated the size available

for the electronic footprint after it was decided to stack the electronics underneath the box. Reduction in the number of laser channels made this simple for the main board. Reduction in the footprint of the FPGA was more of an effort because only commercial off-the-shelf (COTS) devices had been used up to that point. The design task was accomplished in the time allotted and a significant reduction in footprint was realized. The custom FPGA board is designed to plug directly into the main analog board through a single connector.

Figure 4 presents the combined main analog board and custom FPGA board in the deliverable devices after removal of temporary hardware including an LCD and control buttons. The microcontroller is not attached in the Figure and the sensor is shown along side the electronics dust cover and upside down. The two staggered square boards in the foreground are photodetector preamplifiers. The gas sensor enclosure is on the bottom. An RS-232 communications interface is provided via the coaxial SMA cable which routes to a serial-to-USB interface for connection to a netbook computer running an executable LabView VI. A momentary switch disables the lasers before power down.

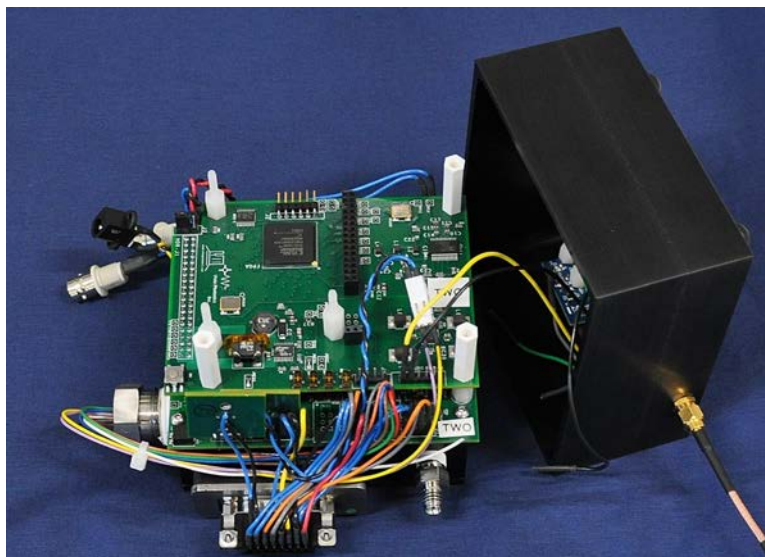


**Figure 4. Sensor version 1.0 electronics.** *The custom FPGA board plugs directly into the main analog electronics board that controls the lasers. The optical sensors are in an enclosure underneath. A plastic dust cover protects the electronics.*

It was determined that using a laser diode at 2703 nm in a simple short optical path offered numerous advantages including wider dynamic range and the potential for a smaller sample volume. Expertise with the wavelength already existed from a Phase II SBIR contract to develop a compact CO<sub>2</sub> sensor for unmanned aerial vehicles (UAVs) with NASA Goddard Spaceflight Center (GSFC). In contrast, the oxygen channel utilized a proprietary path length enhancement approach. The enhancement approach was not an issue for O<sub>2</sub>, where sample volume and response time were less of a concern.

The sensors are fully self contained and run independently with simple 6 VDC power, drawing slightly less than 2 W on average. The FPGA and main boards are capable of running the sensor, acquiring the raw data and converting it to properly demodulated WMS signal. However, they do not provide data analysis, calibration, data logging, or external communication. The microcontroller is essential for providing those functions and a commercial unit was retained in the deliverables.

#### **A. Carbon Dioxide and Water Vapor Channels**

Alpha testing of the combined optical sensors for cross contamination and pressure, temperature, humidity dependence of carbon dioxide precision was accomplished in the vacuum tight optical sensor enclosure incorporating the open path carbon dioxide/humidity channel at 2703 nm, the oxygen channel at 760 nm and the onboard pressure sensor. The enclosure volume is about 200 cm<sup>3</sup> and was primarily determined by the need to accommodate the oxygen path length enhanced cell. A single channel carbon dioxide/humidity sensor would utilize a much smaller sample volume. Temperature is determined by an external thermistor located in a pocket drilled into the aluminum enclosure.

Extensive data were taken for carbon dioxide over a wide range of operating pressures and conditions. The 2703 nm wavelength range contains two absorption features for carbon dioxide with significantly different absorption cross sections, Fig 5. Dynamic range requirements for carbon dioxide detection were accommodated by operating the sensors such that both strong and weak absorption features were accessible in a single laser current-controlled spectral scan, along with a companion water vapor feature. The strong feature is used at low carbon dioxide levels whereas the weak line takes over at high levels. At moderate CO<sub>2</sub> levels the two measurement smoothly transition from one line to the other. In this fashion both low detection limits and wide dynamic range is accomplished for carbon dioxide. Early data for the strong carbon dioxide line were obtained by flow dilution of 8 mmHg CO<sub>2</sub> down to 0 at a constant 400 Torr. The residuals to an exponential fit showed a deviation of less than 0.01 mmHg during

this 24 hour measurement. Similar measurements for water vapor at around 17 % relative humidity (RH) returned a fit deviation of about 0.05 mmHg, or about 0.2 % RH at 25 °C.

The CO<sub>2</sub> channel in the version 1.0 sensor operates in the 2700 nm wavelength range with an open optical path of about 4 cm. Optical absorption spectroscopy provides signal that is linear and quantitative in concentration of the absorbing species *for small absorbances*. As expressed by Beer's law, the signal is directly proportional to the concentration. However, over the range of levels encountered in the PLSS application, the strong line will enter into a non-linear regime of signal versus concentration. Utilizing both absorption features does not entirely eliminate this non-linearity due to the relatively high concentration where the strong line hands off measurement responsibility to

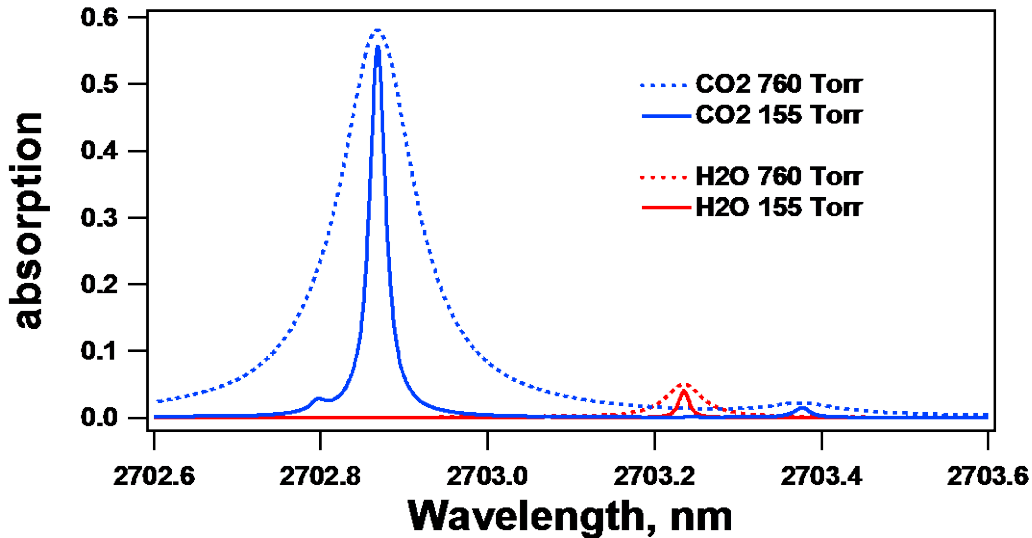


**Figure 5. Absorption Spectrum for CO<sub>2</sub> and water vapor at 2703 nm.** *There are two carbon dioxide lines of different strengths and a water vapor line in the CO<sub>2</sub> channel. The absorption linewidths for the lines are highly pressure dependent.*

the weak line. Figure 5 also shows how the width of the individual absorption features are affected by changing total pressure. The lines get broader as the pressure increases. Version 1.0 sensors were calibrated from 150 Torr up to 800 Torr. Since the WMS measurement technique is sensitive to the absorption line width and the employed current modulation depth, the measured raw signal is necessarily affected by changing pressure. The sensors did not utilize the onboard pressure measurement to adjust the laser modulation depth in order to mitigate pressure effects. Instead, the measured pressure was simply used to correct the measurement error upon deviation from the single pressure where the sensor was calibrated for unity correction (429 Torr, 8.3 psi).

Calibration of the strong carbon dioxide feature was quite complex with quadratic to cubic fits required at individual pressures over the span of concentrations. A range of seven pressures from 155 Torr to 760 Torr was employed. Individual calibration curves were required for each sensor since the curve is a function of modulation depth which is difficult to set identically for both devices. The curvature in an individual fit is due to the non-linear relationship of absorption signal and carbon dioxide concentration at high levels. The signal amplitude is lowest at 760 Torr (the modulation depth was optimum at 150 Torr). Thus, the lasers are very undermodulated at high pressure which degrades the generated signal. The laser modulation depth in version 1.0 was fixed and optimized for a single pressure even though the sensor pressure environment was widely variable. This resulted in less than optimum performance at any pressure that deviates from 150 Torr. Nonetheless, the version 1.0 sensor performance remained high across the entire range. If bidirectional communication between the FPGA and microcontroller could be achieved, the laser modulation depth could be adjusted as a function of pressure and only a single non-linear calibration curve would be required for the strong CO<sub>2</sub> line. This possibility was a major improvement to follow in the version 2.0 sensors.

The weak carbon dioxide feature was linear with concentration at each pressure over the span of concentrations employed even up to 20 % CO<sub>2</sub> at 155 Torr (30 mmHg CO<sub>2</sub> partial pressure) but still required a separate fit at each pressure. In the case of both CO<sub>2</sub> absorption features, the fit coefficients were calibrated as a function of pressure. The pressure measurement is used to obtain the individual appropriate calibration coefficients for both the weak and strong absorption features whether those are linear, quadratic or cubic. The raw count data is then converted to

concentration via those coefficients. In this way, the data analysis and conversion is reduced to two polynomial operations and allows prediction of the fit coefficients outside the bounds of the pressures actually measured. These fit accuracies could be continually improved with more extensive data over a greater range of pressure and concentration alongside finer steps within those ranges. The version 1.0 sensors were not calibrated for variable temperature and their accuracy was degraded at temperatures that deviated from 23 °C.

The early high performance predicted and demonstrated with the loose bread boarded components including the commercial FPGA was preserved in the fully integrated deliverable units. The standard deviation of the carbon dioxide measurements using the strong absorption feature was better than 0.001 mmHg at low carbon dioxide concentrations at 310 Torr. Precision is somewhat better at lower pressures and somewhat worse at the higher pressures (0.003 mmHg at 760 Torr) because of the drop off in signal from the described fixed modulation depth. Similar performance was obtained for both deliverable devices. Both sensors presented essentially equal measurement precision under the same conditions, but also the measured signals were in good agreement and accurate. There was close agreement between the two devices. The inherent sensor response was from 10 % to 90 % within 10 seconds.

### B. Oxygen Channel

There are two regions on either side of 762 nm for oxygen detection accessible with available VCSEL devices. The APLSS oxygen sensors use lasers operating around 760.6 nm. As with the carbon dioxide channel, WMS with second harmonic lock-in detection produces absorption spectra with qualitative second derivative lineshapes. The VCSEL devices tune much farther for a given change in temperature. The tuning rate with current is likewise much faster than that of laser diodes. This results in much less amplitude modulation associated with the desired wavelength modulation making oxygen detection easier. Data obtained from the path length enhanced oxygen sensor (about 150 cm in a sample cell less than 4 cm across) provides a standard deviation of about 0.2 %. The oxygen channel was preserved in the version 2.0 sensors but has been eliminated in the version 2.5 device in order to get further towards the version 3.0 architecture which must be much smaller for EMU compatibility.

### C. Unit conversion and calibration using Netbook computer

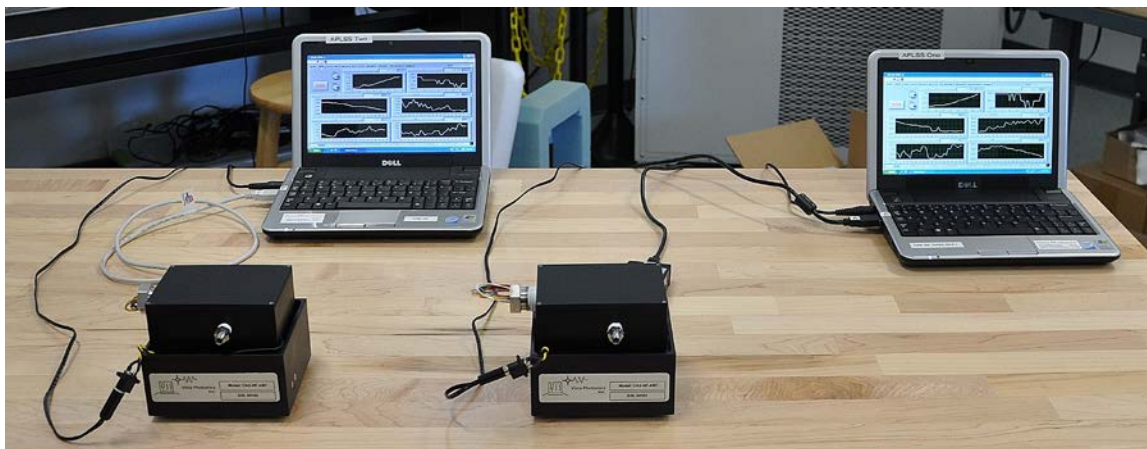


**Figure 6. Version 1.0 sensors before delivery.** *Both sensors offer equivalent performance for the three gases measured. Netbook computers were required to implement the complex calibration in the version 1.0 sensors. The computers were not simply logging data, they converted the raw engineering units into useful concentration data after acquiring pressure readings from the onboard sensors.*

At the time of the version 1.0 sensor delivery the species calibrations for all three gas channels were employed through the use of a netbook computer to take the raw sensor output in counts over a serial port and convert to concentrations. The two version 1.0 sensors are shown with netbook computers reporting the measured gas concentrations in Fig. 6 immediately prior to delivery. The netbook also logs appropriate converted data along with temperature and pressure data. It has since proven feasible to incorporate the calibrations directly into the microcontroller such that the output is in concentration instead of counts for each gas.

### III. Optical Sensor Version 2.0

The version 1.0 sensors were installed and tested in the APLSS 1.0 bread board in October, 2011. Good measurement agreement with several other carbon dioxide sensors accessible on the bread board was achieved over the course of several days with Vista Photonics' personnel participating. This testing occurred after the primary demonstration of the APLSS 1.0 breadboard and before transition to the present 2.0 version. Several changes that would improve the devices were highlighted by this testing. It was learned that the pressure sensor inside the optical enclosure was susceptible to failure at the high humidity levels encountered. Since the advanced PLSS will itself employ its own state-of-the-art pressure sensor, the version 2.0 optical sensors use this measurement communicated over a serial interface instead of using a separate onboard pressure sensor. However, a better pressure sensor was implemented in the version 2.0 sensors as a precaution should onboard measurement become necessary in the future.

A second desired improvement was to separate the oxygen and carbon dioxide channels from inside the same enclosure sample volume. Oxygen sensing with the path length enhanced architecture is the determining factor in the 200 cm<sup>3</sup> volume of the optical sensor enclosure. The open path carbon dioxide channel was built as a sub-assembly and then mounted inside the optical sensor enclosure. The enclosure simply functions as a small vacuum chamber and sample cell. The enclosure was added due to the need to separate the main electronics from the optical sensors, which are to be in contact with the sample gas. Even so, the sensors themselves require electrical wiring for the laser and photodetector and this wiring is in contact with the sample gas. The carbon dioxide/humidity sensor alone could present a significantly reduced footprint and 2 cm<sup>3</sup> volume if separated from the oxygen channel, which would itself only occupy 50 cm<sup>3</sup>. The common enclosure also exposes the laser diode, VCSEL and photodetectors to what could eventually be a pure oxygen environment. The version 2.0 sensors locate the electrical leads for the laser diode, VCSEL and the photodetector for the carbon dioxide channel outside of contact with the sample gas. Only the electrical leads of the photodetector for the oxygen channel remains in contact with the sample gas and they carry only about 30 microwatt.



**Figure 7. Integrated Version 2.0 sensor.** *Optical and electronic layout after full conversion to 2.0 architecture. An RS-485 bi-directional interface and power supply board compatible with the APLSS 2.0 system has been added.*

The original delivered 1.0 devices were returned for upgrade to the new 2.0 version in March 2012 and the new devices delivered in July 2012. Several of the improvements are evident in the Figure 7. The aluminum block on the right side of the enclosure is the new carbon dioxide and water vapor channel with both the laser diode and photodetector removed from contact with the sample gas. The new oxygen channel is in the cubic enclosure on the left of the figure with the vacuum electrical feed through. The other wires on the enclosure are for the VCSEL, which is located out of contact with the sample gas. The sensor volume has been rearranged for accommodation within the available space of the APLSS 2.0 system. This resulted in a more rectangular shape than the previous cubic shape of the 1.0 devices. Additional changes involved locating a single electrical connector and both gas line connectors (inlet and outlet) on the same side of the sensor enclosure. The gas connectors were custom made to transition from the APLSS preferred style to the compression tube fittings utilized inside the sensor. Upgraded electronics were also produced during that period before delivery of the version 2.0 sensors that included a new

main analog board and a redesigned custom FPGA board. One of the photodetector preamplifiers was also relocated onto the main analog board. The RS-232 interface already on the microcontroller board was connected through a new custom RS-485 interface offering bidirectional communication. This allows sending of multiple commands to the sensor as well as providing for an external pressure measurement. The microcontroller has been, likewise, upgraded to eliminate an unnecessary compact flash card reader. The version 1.0 sensors operated off of a 6 VDC power supply while the upgraded 2.0 sensors operate from the APLSS supplied 16 to 34 VDC power. That power conditioning was added to the same board containing the RS-485 interface.

In addition to the reduced sample volume, increased safety, and upgraded electronics improved sensor performance was realized by making the laser diode modulation depth a pressure-dependent variable. The 1.0 sensors operated with a fixed modulation depth (wavelength excursion turning points) although the absorption linewidth is a function of pressure. Consequently, signal is degraded at pressures other than the one for which the sensor is optimized. Figure 8 shows how the signal changes with pressure for a fixed modulation depth. Of course, the calibration takes care of this in terms of the concentration reading reported to the end user. However, the calibration cannot retrieve the lessened performance (reduced precision) for pressures where the modulation depth is not optimal. Such variation can approach a factor of three worse precision at the highest pressures. The Figure also shows the sensor readings for the case where the modulation depth is optimized for the actual pressure. Very little variation is found which would greatly reduce the computational overhead employed in the version 1.0 sensor pressure compensation (which was complex enough to require the netbook computer). A variable modulation depth based on the onboard pressure reading or an external measurement would essentially eliminate the sensor pressure dependence. Thus, the raw sensor output would be nearly pressure independent requiring little clean up from the calibration algorithm. This approach would require the FPGA to employ a feedback loop of modulation depth based on the pressure sensor reading. Vista Photonics had not employed this approach before on an autonomous sensor and appropriate safeguards to protect the laser diode were developed.

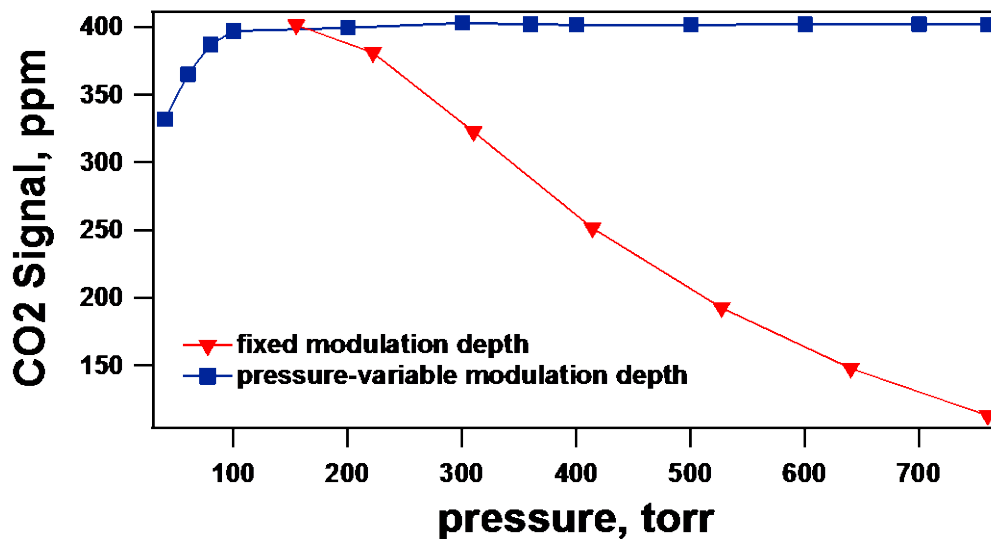


**Figure 8. Adjusting the modulation depth increases sensor performance.** *The version 1.0 sensors simply corrected for pressure variation away from the optimized level as shown by the fixed modulation depth trace. Sensor performance dropped off away from the optimum pressure. In contrast, the version 2.0 sensors adjust their operation as a function of pressure to maintain their high performance across the entire required pressure range.*

The modulation depth has to be changed to keep the carbon dioxide signal as constant as possible under changing pressure conditions at a fixed mole fraction (parts-per-million by volume). The signal still drops if the pressure is less than 200 Torr even with optimized modulation depth as the line goes from primarily pressure broadened to Doppler broadened. The line doesn't narrow up and increase in height for pressures below 200 Torr. The limit requirement for the sensors is 150 Torr, so the data will have some error, if left uncorrected, at the very lowest pressures by the microcontroller where a tiny bit of precision will be lost. However, the sensors were previously optimized for 150 Torr in Phase III so that at every higher pressure the signal had degraded precision. Thus, the upgraded version 2.0 sensors will have higher precision at every pressure at which they operate. Raw data were used to construct the required modulation depth versus pressure in a fully closed loop control such that the

system would take the known pressure and adjust the modulation depth automatically. The microcontroller informs the FPGA of the pressure and the FPGA uses the information to drive the laser diode appropriately. Full bi-directional communication has been implemented between the two digital devices. The version 1.0 sensors had uni-directional communication only. This was the most complex task for implementing the desired version 2.0 improvements. The two upgraded sensors are shown in Fig. 9 prior to delivery in July 2012.

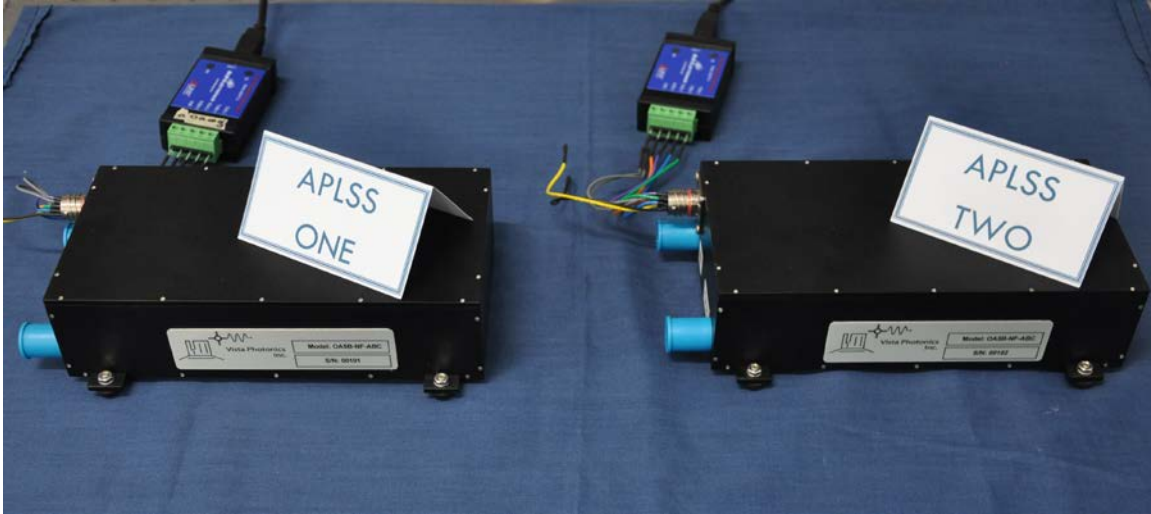


**Figure 9. Version 2.0 sensors before delivery.** The two version 1.0 sensors were upgraded to version 2.0 and are geometrically and electrically compatible with the APLSS 2.0 system.

#### IV. Optical Sensor Version 2.5

An advanced PLSS 2.0 sensor (SN103) has been upgraded to run on software like that of the Multi-Gas Monitor currently exceeding 2 years of on-orbit operation. The software implements wavelength locking of the laser diode so that the desired signal measurement occurs in the same part of the spectrum at all times, thus eliminating drift. The APLSS 2.5 sensor successfully locks if CO<sub>2</sub> signal is greater than about 0.085 mmHg at 4.3 psia. That threshold lock level scales roughly with total pressure since the sensor's fundamental metric is parts-per-million (ppm). The locking threshold does not mean that accurate measurements are not made below that level, rather that the sensor does not update or drive to its default peak locations when the signal-to-noise ratio is too low. The sensor essentially goes to free running at very low concentrations but re-locks once levels have increased. Further, water vapor alone is sufficient for locking at high enough levels. At 4.3 psia the sensor can lock accurately with about 1.7 mmHg of water vapor (7 % RH at 25 °C) even if CO<sub>2</sub> is below the sensor detection limit.

The sensor was configured and calibrated in the laboratory using an RS-232 interface compatible with the latest corresponding MGM LabView software which was more sophisticated than the old software compatible with the 2.0 sensor RS-485 interface. The advanced PLSS 2.5 sensor was switched later to the required RS-485 interface. The upgraded sensor was, thereby, delivered as plug-and-play compatible with the extant software on the NASA JSC sensor test rig. The standard software command set was not changed so that NASA testing could proceed without programming changes. However, the microcontroller has been configured to respond to additional commands than before which provide more internal sensor parameters including the measured spectrum. Utilization of those commands requires additional programming on the NASA side of the interface. Running as fast as possible, the sensor streams data between 1.5 and 2.2 Hz depending on how many signals are present in the spectrum at any given time. The sensor averaging parameters for both carbon dioxide and water vapor have been set to provide a 0 to 90 % response of 8 seconds.

The APLSS 2.5 sensor fundamental measured concentration parameter is ppm by volume. In contrast, the EVA needs are defined by the carbon dioxide partial pressure (mmHg). CO<sub>2</sub> partial pressure is obtained by multiplying the ppm (mole fraction) by the total pressure. Because the sensor performance definitions like precision, accuracy and detection limit are obtained in ppm, they necessarily scale (get worse) with increasing total pressure.

The difficulty in merging the ppm nature of the measurement with the partial pressure definition of the requirements is compounded by VPI's use of two carbon dioxide absorption features of different strength. However,

the separate lines allow meeting the wide dynamic range of concentrations encountered over the total pressure range of 3 to 25 psia (150 to 1300 Torr) with CO<sub>2</sub> partial pressures from 0.1 to 30 mmHg. Figure 10 shows the CO<sub>2</sub> partial pressure returned by the sensor in mmHg after conversion from its native ppm measurement. The data trace spans partial pressure ranges that include both carbon dioxide measurements. Bumps and dips in the trace are caused by the clearing out of gas lines as one calibrated standard CO<sub>2</sub> mixture after another is presented to the sensor. In the first part of the trace, the total pressure is kept at the primary design level of 4.3 psia while the concentration of carbon dioxide is stepped up and down. In the second part, the CO<sub>2</sub> concentration (ppm) is kept constant while the total pressure is stepped at several waypoints between 4.3 and 15.1 psia. Both approaches result in variable CO<sub>2</sub> partial pressure.

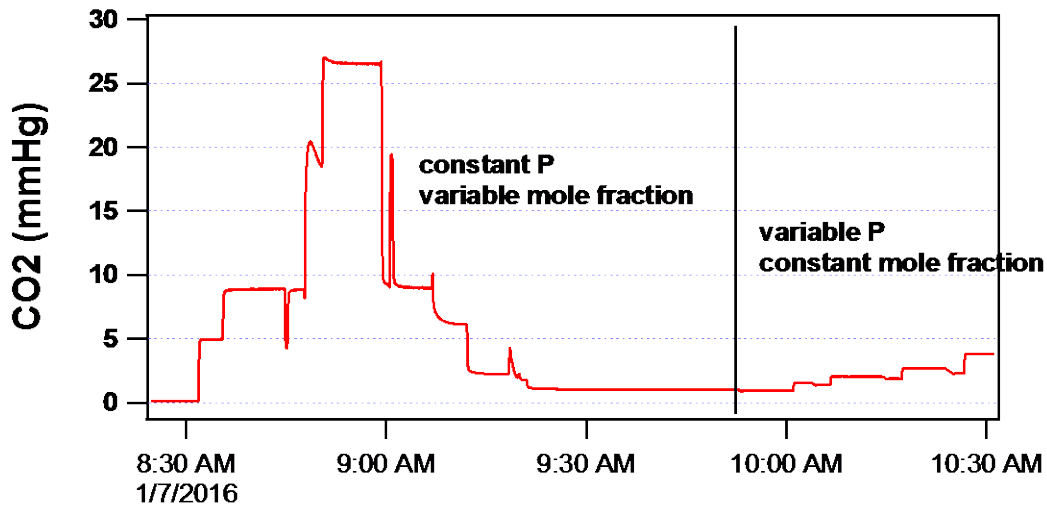


**Figure 10. Carbon dioxide partial pressure challenges.** After calibration, the version 2.5 sensor was presented with variable partial pressures of carbon dioxide by varying the fractional concentration and the total pressure.

Carbon dioxide calibration on the weak absorption feature was accomplished with two concentration points since the output is sufficiently linear. The weak feature measurement is not used in the sensor output unless CO<sub>2</sub> exceeds 35,000 ppm. The strong feature is more difficult to calibrate because its Beer's law output is non-linear. Initially, the output was calibrated against a LiCor device that had itself been calibrated up to 40,000 ppm. The APLSS 2.5 and LiCor sensors were daisy chained and presented a smoothly varying concentration from 0 to 40,000 ppm over the course of several hours from two certified standards. The APLSS 2.5 sensor then used the LiCor measurement in ppm for conversion of its engineering units to ppm. Over the course of a subsequent month the two sensors were run together through various challenges and remained in close agreement. Two additional standards were received a month later with around 1 % and 0.5 % carbon dioxide and presented to both sensors. The sensors were in good agreement with one another but read much lower than expected based on both new certified concentrations. After recalibrating the LiCor with the 1 % solution and testing it with the previous 4 % standard it became clear that the LiCor sensor was not sufficiently accurate over this range to transfer calibration measurements to the APLSS 2.5 sensor.

The APLSS 2.5 sensor has been designed from the beginning of the upgrade to have a primary calibration at 4.3 psia and 28 °C, which is then corrected for changes in pressure and temperature over the required respective ranges. Pressure and temperature corrections are simple factors normalized to the default conditions. Consequently, a recalibration can be obtained just at the default conditions and those changes will be applied throughout the operating envelope of the device. That feature was utilized with the available calibrated CO<sub>2</sub> standards (0, 385, 4939, 10010, 40250 ppm) and the new, LiCor-independent, calibration parameters were acquired and implemented on the sensor. The neat, certified, standards were presented to the sensor without flow dilution to eliminate mixing errors. That new calibration was applied before the data of Figure 10 was obtained.

Figure 11 shows the results of testing the sensor with the same certified standards after calibration. In a sense, the data just documents that the sensor returns the same response when presented with the same concentration at a later time, so the data demonstrates sensor stability. Further, it shows that the inherent non-linearity of the raw sensor output has been well-linearized by the calibration. The solid line in Figure 11 shows an ideal response (without error) based on calculation of the partial pressure from the certified concentration and measured total

pressure. The symbol markers are the sensor response.

Figure 12 shows like data that demonstrates the validity of the total pressure correction. In the Figure, partial pressure is increased simply by increasing the total pressure at a fixed concentration in ppm (at several points between 4.3 and 15.1 psia). This is much more of a challenge for the sensor since it must make an accurate ppm measurement at the various total pressures in order to return the right answer. Again, the solid line shows ideal response and the symbol markers are the sensor response. Error is minimal and within the 0.15 mmHg specification for partial pressures below 8 mmHg.

The sensor is calibrated up to 25 psia. The sensor will ultimately incorporate more calibration points between 10,000 ppm and 40,000 ppm which are being acquired during testing at NASA JSC. The sensor can provide the raw engineering output data from the additional gas standards available to NASA through the software interface. An updated calibration can be implemented on the sensor by switching out the microcontroller or uploading new software.

The highest partial pressure at the lowest total pressure corresponds to 200,000 ppm (30/150). The lowest partial pressure at the highest total pressure corresponds to 77 ppm (0.1/1300). The actual dynamic range required based on the sensor's fundamental measured parameter is not the factor of 300 between 0.1 and 30 mmHg but, rather, the factor of 2,600 between 77 and 200,000 ppm. That range is accommodated by using the two CO<sub>2</sub> lines available within the rapid scanning range of the laser. Figure 13 shows how those lines are selected as a function of total pressure and partial pressure. The regions bounded by the blue lines have higher precision, marked "best", though the actual standard deviation within those bounds is still a function of partial pressure. Between the two regions (where CO<sub>2</sub> falls between 35,000 and 40,000 ppm) the two line measurements are averaged. At the nominal suit pressure of 4.3 psia, the lines hand off at around 7.8 mmHg partial pressure of CO<sub>2</sub>. The region bounded by the red lines has less precision but the ppm concentration is too high to use the strong carbon dioxide line. As a reference, the *precision* at around the partial pressure of 30 mmHg and 14.7 psia is about 0.02 mmHg for the blue region and 0.08 mmHg for the red region.

The sensor has been calibrated on the strong CO<sub>2</sub> line up to 40,000 ppm and on the weak line up to 200,000 ppm. This combination provides the needed range up to 30 mmHg between 3 and 25 psia. The weak line is not used at all above about 900 Torr since the strong line is sufficient to determine 30 mmHg and less at those pressures. The sensor always needs to be provided the correct pressure by an external sensor over the RS-485 interface as the on-board pressure sensor is not in contact with the sensed fluid.

The sensor has been calibrated for water

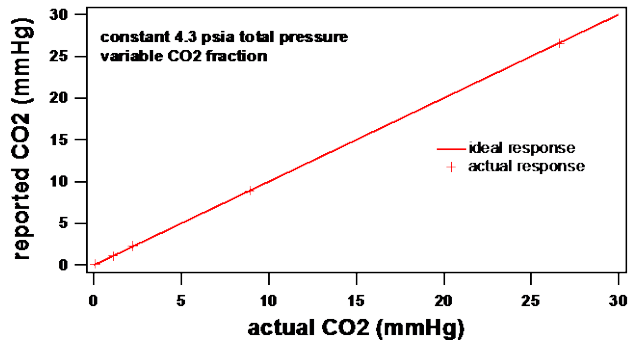


**Figure 11. Carbon dioxide partial pressure challenges.** CO<sub>2</sub> measured partial pressure versus actual for variation introduced by changing mole fraction at constant total pressure.

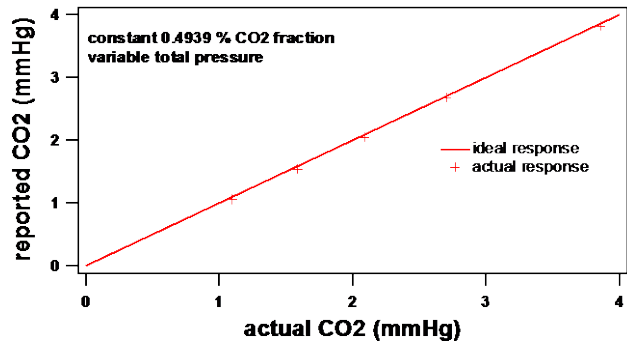


**Figure 12. Carbon dioxide partial pressure challenges.** CO<sub>2</sub> measured partial pressure versus actual for variation introduced by changing total pressure at constant mole fraction.

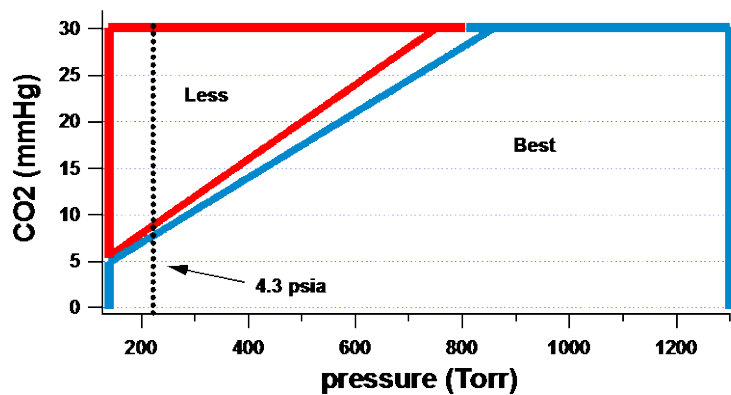


**Figure 13. Regions of low and high precision for CO<sub>2</sub>.** The use of two CO<sub>2</sub> metrics determined by mole fraction leads to regions of higher and lower precision that are dependent both on partial pressure and total pressure.

vapor at 4.3 psia and the pressure correction determined and applied for the 3 to 25 psia range. Water vapor measurement precision is about 0.01 mmHg at 4.3 psia which equates to better than 0.05 % RH. Water vapor detection limits at 4.3 psia are about 1.8 % RH at 25 °C. The precision scales (becomes worse) linearly upon increasing pressure with an additional span of two included so that at 15 psia about 0.05 mmHg resolution is achieved. The water vapor detection limit is below 5 % RH at 25 °C up to about 10.2 psia. At higher pressures up to 15.1 psia the detection limit is between 5 and 7 % RH at 25 °C. Figure 14 shows data simultaneously acquired for CO<sub>2</sub> and H<sub>2</sub>O at 4.3 psia after implementing the calibrations. Ambient air was blended with a certified standard of CO<sub>2</sub> at 4.025 % so that when CO<sub>2</sub> is increased, H<sub>2</sub>O is decreased. The CO<sub>2</sub> signal in the trace is determined by the algorithm which decides which CO<sub>2</sub> line to use or to use both. The highest level in the Figure was purposely chosen so that both CO<sub>2</sub> measurements are combined/averaged. Worst case precision for 4.3 psia total pressure at the concentrations presented in the Figure is about 0.015 mmHg for CO<sub>2</sub> at 8.8 mmHg and about 0.01 mmHg for H<sub>2</sub>O at 1.8 mmHg. Note that the red CO<sub>2</sub> trace does not quite reach zero, corresponding to 0.085 mmHg when only ambient air is being sampled. That low, near-zero, concentration is sufficient for line locking at 4.3 psia.

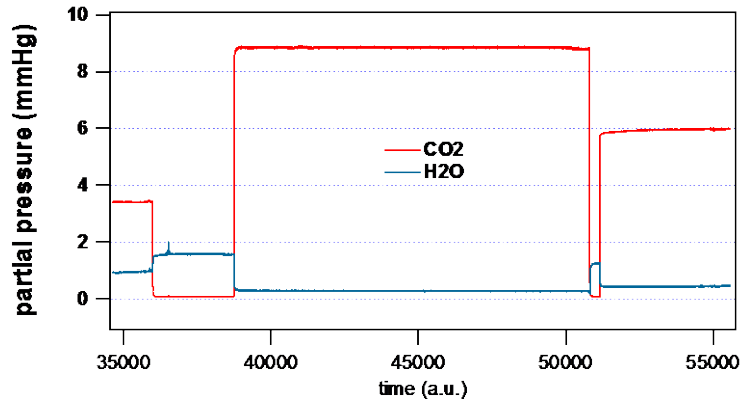


**Figure 14. Simultaneous carbon dioxide and water vapor measurement.** CO<sub>2</sub> and H<sub>2</sub>O measured together with single laser channel while both concentrations are varied. Both measurements are stable to about 0.01 mmHg at 4.3 psia.

Vista Photonics' optical breath gas sensor version 2.5 is being tested on the Gas Sensor Test Stand shown in Figure 15. The test stand was designed and built by the Space Suit and Crew Survival Systems Branch at the NASA Johnson Space Center for testing and characterizing the performance of gas sensors for portable life support systems (PLSS). The test stand provides a fully-automated capability for delivering a gas mixture of controlled N<sub>2</sub> and CO<sub>2</sub> concentrations (by mass), mixture static and dew-point temperatures, and mixture mass flow rate to a gas sensor under test. Additionally, the stand contains a vacuum chamber in which the sensor resides during test, which allows for testing of the sensor at the typical sub-ambient static pressures and pressure differentials under which PLSS gas sensors are expected to operate. Closed-loop pressure controllers maintain a desired internal sensor pressure with respect to sensor ambient during test to replicate the range of gas densities encountered during PLSS operations. The test stand provides fully automated control, monitoring, collection, and logging of all test stand and sensor operational parameters and data, and also protects against over-pressurization, over-voltage, and over-current conditions. Lastly, a Picarro Gas Analyzer is used to provide verification of the CO<sub>2</sub> concentration being delivered to the gas sensor under test.



**Figure 15. NASA JSC Gas Sensor Test Stand.**

## V. Optical Sensor Version 3.0

The next development stage for the optical carbon dioxide and water vapor sensor will require substantial reduction in total volume while providing a path way towards a radiation tolerant design. Volume reduction is being accomplished by eliminating the oxygen channel altogether. It is expected that reorienting the optical cell and tighter packing of the electronics will allow meeting the required reduction in volume. In parallel, a new FPGA is being tested as part of the version 3.0 sensor. The FPGA has a radiation tolerant equivalent product offering. The evaluation board has been tested functional and changes to a simple program made for proof-of-principle. All the parts to test the functioning are in place. The device has been tested for compatibility with the required advanced PLSS version 2.5 sensor operating algorithm. The steep learning curve for using a second FPGA copy to run a soft-core processor (Leon 3 or 8051) has continued with the intent to replace the Tern microcontroller presently in use on the advanced PLSS sensors. There is the possibility that the present non-radiation tolerant FPGA can be replaced by the new one and that a denser version (more gates) may be able to replace both the separate FPGA and

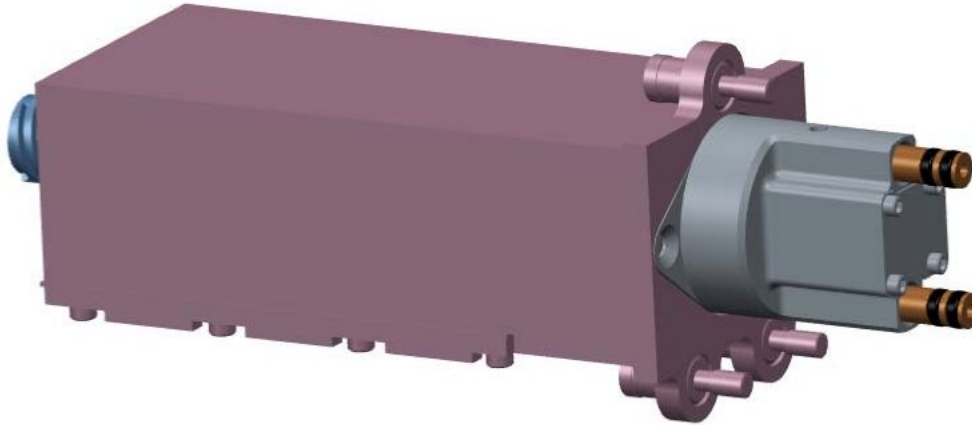


**Figure 16.** Package outline for advanced PLSS 3.0 sensor. *CO<sub>2</sub> and H<sub>2</sub>O sensor must be much smaller for compatibility with EMU. Longest dimension is about 6”.*

microcontroller in a single radiation tolerant chip. This will go a long way towards replacing the electronic functionality on a point-by-point basis while providing a path way to meet the APLSS 3.0 size and volume requirements. Table 1 compares and contrasts performance and physical metrics for the four evolutions of the advanced PLSS CO<sub>2</sub> and water vapor sensor.

Version	1.0	2.0	2.5	3.0
Pressure range	3 - 15.5 psia	3 - 23	3 - 25	3 - 25
Water vapor	0.2 % RH	0.2 %	0.05 %	
Response (90 %)	10 s	10	8	8
Data rate	6.7 s	2.1	0.7	
Sensor volume	72 in <sup>3</sup>	55	40	19
Oxygen included	Yes	Yes	No	No
Radiation tolerant	No	No	No	Yes

Version 3.0 of the sensor is being designed to be backwards compatible with the EMU space allocation as shown in the rendering of Figure 16. Dimensions are about 6.1” x 2.1” x 1.5”. However, the sensor will now be capable of additional measurement of water vapor within the volume of the previous IR transducer. This may be useful for early warning of imminent condensing conditions.

## VI. Conclusion

An integrated optical architecture utilizing lessons learned and techniques advanced on several NASA SBIR projects has been developed for use in the emerging advanced PLSS for EVA. The first version of the sensors proved the value of the optical approaches employed and resulted in a compact, rugged, design. Various design improvements were made in the second version that provided a more suitable geometry for the EVA application

while increasing sensor performance. Sensor power draw was also reduced and full bi-directional communication added in the second version. Further, the complex calibration previously done through a netbook computer was offloaded onto the internal microcontroller. The serial communication is now used primarily to acquire the concentration data. A version intermediate to 2.0 and 3.0 implemented wavelength stabilization and locking as well as a more efficient communications interface between the digital electronics. Water vapor measurement precision was also improved. That version 2.5 upgrade resulted in a carbon dioxide and water vapor measurement rate at over 1.5 Hz, ten times faster than the original design. In future work, a version 3.0 sensor design already in progress could see a nearly 50 % decrease in volume by better arrangement of the carbon dioxide sample cell and emerging electronics while offering a path way to a radiation tolerant design.

### **Acknowledgments**

The authors wish to acknowledge support from the National Aeronautics and Space Administration through contracts NNJ11HB99P, NNX10CA95C-IIE, NNJ12HE04P and NNX15CJ53C.